

Article

The Effective Combination of Humic Acid Phosphate Fertilizer Regulating the Form Transformation of Phosphorus and the Chemical and Microbial Mechanism of Its Phosphorus Availability

Qizhong Xiong^{1,2,3,*}, Shaojie Wang^{1,2,3}, Xuwei Lu^{1,2,3}, Yating Xu^{1,2,3}, Lei Zhang^{1,2,3}, Xiaohui Chen^{1,2,3}, Gang Xu^{1,2,3}, Da Tian^{1,2,3}, Ligan Zhang^{1,2,3}, Jianyuan Jing^{1,2,3} and Xinxin Ye^{1,2,3,*}

¹ Anhui Province Key Laboratory of Farmland Conservation and Pollution Prevention, College of Resources and Environment, Anhui Agricultural University, Hefei 230036, China

² Anhui Province Engineering and Technology Research Center of Intelligent Manufacture and Efficient Utilization of Green Phosphorus Fertilizer, Anhui Agricultural University, Hefei 230036, China

³ Key Laboratory of JiangHuai Arable Land Resources Protection and Eco-Restoration, Ministry of Natural Resources, Anhui Agricultural University, Hefei 230036, China

* Correspondence: qzxiong@ahau.edu.cn (Q.X.); yexx@ahau.edu.cn (X.Y.)

Abstract: In the process of phosphate fertilizer production, adding humic acid to produce humic-acid-value-added phosphate fertilizer can improve fertilizer efficiency and promote crop growth. Although studies have primarily focused on investigating the impact of humic acid's structure and function on phosphorus availability in humic-acid-added phosphate fertilizers, there is limited research on the regulatory effects of phosphorus fertilizer structure and the synergistic mechanisms involving microorganisms. Therefore, this study aimed to examine the chemical and biological mechanisms underlying the increased efficiency of humic-acid-added phosphate fertilizers by implementing various treatment processes. These processes included physically blending humic acid with phosphate fertilizer (HA+P), chemically synthesizing humic acid phosphate fertilizer (HAP), using commercially available humic acid phosphate fertilizer (SHAP), employing ordinary potassium phosphate fertilizer (P), and implementing a control treatment with no phosphate fertilizer (CK). Investigating the synergistic mechanism of humic-acid-added phosphate fertilizers holds significant importance. The results showed that during the preparation of HAP at high temperature, a new absorption peak appeared at 1101 cm^{-1} , and a new chemical bond -O- was formed. The hydroxyl fracture in humic acid combined with phosphoric acid to form a phosphate ester (P-O-C=O) structure. HAP residues were concentrated on the surface and loaded with more soil minerals. The content of highly active oxygen-containing functional groups—such as aromatic C-O, carboxyl/amide carbon and carbonyl carbon—increased significantly, while the content of alkyl carbon, oxyalkyl carbon, and aromatic carbon decreased. Upon combining humic acid with potassium phosphate, the carboxyl group and calcium ions formed the HA-m-P complex, increasing the content of soluble phosphate (H_2PO_4^-) in the soil by 1.71%. Compared to HA+P treatment, HAP treatment significantly increased the soil's available P content by 13.8–47.7% ($P < 0.05$). The plant height, stem diameter, and above-ground biomass of HAP treatment were increased by 21.3%, 15.31%, and 61.02%, respectively, and the total accumulations of N, P, and K nutrient elements were increased by 6.71%, 31.13%, and 41.40%, respectively, compared to the control treatment. The results of high-throughput sequencing showed that the rhizosphere soil of HA+P and HAP treatment was rich in bacterial groups, the soil microbial structure was changed, and the bacterial community diversity was increased under HAP treatment. The number of genes encoding phytase and alkaline phosphatase associated with organophosphorus dissolution increased by 3.23% and 2.90%, respectively, in HAP treatment. Humic acid phosphate fertilizer forms phosphate esters in the process of chemical preparation. After application, the soil's microbial community structure is changed, and soil enzyme activity related to phosphorus transformation is improved to promote tomatoes' absorption of soil nutrients, thus promoting tomato plant growth and nutrient accumulation.



Citation: Xiong, Q.; Wang, S.; Lu, X.; Xu, Y.; Zhang, L.; Chen, X.; Xu, G.; Tian, D.; Zhang, L.; Jing, J.; et al. The Effective Combination of Humic Acid Phosphate Fertilizer Regulating the Form Transformation of Phosphorus and the Chemical and Microbial Mechanism of Its Phosphorus Availability. *Agronomy* **2023**, *13*, 1581. <https://doi.org/10.3390/agronomy13061581>

Academic Editor: Wei Zhang

Received: 16 May 2023

Revised: 6 June 2023

Accepted: 8 June 2023

Published: 11 June 2023



Copyright: © 2023 by the authors. Licensee MDPI, Basel, Switzerland. This article is an open access article distributed under the terms and conditions of the Creative Commons Attribution (CC BY) license (<https://creativecommons.org/licenses/by/4.0/>).

Keywords: humic acid; humic acid phosphate fertilizer; chemical structure; microflora; phosphorus availability; synergistic mechanism

1. Introduction

In global agricultural production, phosphorus (P) ranks as the second-most limiting nutrient for crop yield after nitrogen [1]. As an essential nutrient for crop growth, P serves various crucial functions throughout the plant's lifecycle [2,3]. The application of phosphate fertilizers (such as TSP, SSP, FCMP, DAP, MAP) has been proven to promote crop growth, development, and ultimately to increase yield [4–7]. However, after the application of phosphate fertilizer, soil buffer capacity decreases, and phosphorus is absorbed by soil colloidal particles and metal ions, gradually forming non-available phosphate that is difficult for crops to absorb and utilize [8,9] because of the poor mobility of phosphorus in soil [10]. At present, the utilization rate of phosphate fertilizer in China is about 10–20% [11]. In pursuit of high yield, excessive application of phosphate-based fertilizer will lead to the depletion of phosphorus reserve resources and cause environmental problems [12]. Therefore, improving the use efficiency of phosphate fertilizer in agricultural production systems will still be a major challenge in the future. Increasing the solubility and availability of soil and improving the utilization efficiency of phosphate fertilizer are the key to solving the persistent and global phosphorus crisis. The development of highly efficient phosphate fertilizers through microbial, physical, and chemical modification methods holds promising potential in alleviating the global phosphorus crisis [13–15].

Humic acid, a naturally occurring macromolecular organic substance, is formed through the decomposition and transformation of animal and plant remains by a variety of microorganisms as well as through various physical and chemical processes in nature [16,17]. It exists widely in nature and plays an important role in improving soil health and plant growth [18]. The basic structure of humic acid macromolecules is an aromatic ring and a lipid ring, and the rings are connected with carboxyl, hydroxyl, carbonyl, and other active functional groups, so it has a variety of functions. For example, humic acid can increase the availability of phosphorus in soil and fertilizer by chelating metal ions [19] and competing with phosphate for adsorption sites on soil particles' surfaces [20–22]. Humic acid has positive effects on crop seed germination, seedling root and stem growth, enzyme activity in soil [23], crop yield and quality, etc. Therefore, humic acid is always applied in large quantities to the soil.

In recent years, ordinary phosphate fertilizer (organic phosphate fertilizer) combined with trace plant biohormones has become an emerging method of improving the efficiency of phosphate fertilizer [24], and the fertilizer made is called value-added phosphate fertilizer. Humic acid has become a popular carrier in the development of synergistic fertilizers based on its structural characteristics and good effects [25]. The effect of humic acid on phosphate fertilizer is closely related to its dosage, type, functional group structure, and molecular weight [26]. Jing et al. [27] showed that humic acid phosphate fertilizer prepared at high temperature increased the contents of carboxyl groups and low molecular components, but reduced hydrophilicity or inappropriate addition amount would lead to insignificant synergy of humic acid with phosphate fertilizer and crops. Through soil column experiments, Wu et al. [28] found that humic acid limited the adsorption of PO_4^{3-} by goethite to varying degrees, and higher concentrations of humic acid usually led to a lower adsorption capacity of goethite. However, the chemical structure, molecular morphology, binding mechanism, and biological synergistic mechanism of humic acid organic phosphate fertilizer are still unclear in view of the current technological level. Based on this phenomenon, combined with the properties of humic acid, we analyzed the structural changes after the chemical combination of humic acid and phosphate fertilizer, and the synergistic mechanism was explored from the chemical and biological perspectives to explain the growth and nutrient absorption of tomato plants.

Therefore, this paper delves into different combination processes of humic acid and phosphate fertilizer regulating the transformation of phosphorus and improving the effectiveness of phosphorus and the microcosmic mechanism by using advanced characterization techniques. It has important research significance for improving the crop absorption and utilization efficiency of phosphorus, contributing to the production of the phosphate fertilizer effect, promoting green agricultural production and ecological environment protection.

2. Methods

2.1. Preparation for Materials

Extracting humic acid (HA) from weathered coal. Firstly, the ground and screened weathered coal were mixed evenly with 0.5 M NaOH at a solid–liquid ratio of 1:10. After the solution was stirred at room temperature for 24 h, the impurities were removed via centrifugation at 8000 r/min for 10 min to obtain humic acid solution. The pH of the humic acid solution was adjusted to 1 with 6.0 M HCl, and the solution was left standing for 24 h. After centrifugation at 8000 r/min for 10 min, the supernatant was discarded to obtain the crude extracted humic acid. Then, the crude extracted humic acid was mixed evenly with 0.1 M HCl+ 0.3 M HF solution; the solid–liquid ratio was always 1:10, and the inorganic substances were removed by shaking for 24 h and washing 3 times to purify the crude humic acid. Similarly, Cl^- was removed by washing with deionized water 3 times at a solid–liquid ratio of 1:10. Finally, the purified humic acid was freeze-dried to obtain humic acid powder, which was dried and stored for later use.

Preparation of physical blended humic acid phosphate fertilizer (HA+P) and chemically synthesized humic acid phosphate fertilizer (HAP) for the test fertilizer. Humic acid material accounting for 10% of the total mass of phosphoric acid solution and potassium hydroxide (the molar to mass ratio of phosphoric acid to potassium hydroxide was 1/2) was added to the phosphoric acid solution and stirred well. Then, potassium hydroxide was added—followed by rapid stirring, grinding, sieving, and drying for preservation—to obtain the humic acid phosphate fertilizer used in the test through high temperature acid–base reaction. Humic acid cracking small molecules may be combined with phosphoric acid to form new substances through acid–base neutralization reactions. The phosphate fertilizer made of humic acid is codenamed HAP, and the ordinary phosphate fertilizer without humic acid added, codenamed P. The ordinary phosphate fertilizer P was physically blended with the same mass of humic acid material as above to obtain the physical blending of humic acid phosphate fertilizer used in the test, recorded as HA+P.

2.2. Plant Material and Test Methods

2.2.1. Materials and Test Procedure

The pot trials were conducted in the experimental greenhouse of Anhui Agricultural University's Nongcui Garden, Anhui Province, China. The test soil was taken from the 0–20 cm cultivated layer of the 3-year cultivated shed in the vegetable science and technology demonstration garden in He County, Anhui Province, China. Basic physical and chemical properties of the soil were as follows: pH: 6.66, organic matter: $19.10 \text{ g}\cdot\text{kg}^{-1}$, total nitrogen: $1.20 \text{ g}\cdot\text{kg}^{-1}$, available phosphorus: $76.0 \text{ mg}\cdot\text{kg}^{-1}$, available potassium: $443 \text{ mg}\cdot\text{kg}^{-1}$.

Five treatments were set up in the experiment: (1) no phosphate fertilizer treatment (CK); (2) common phosphate fertilizer treatment (P); (3) chemical synthetic humic acid phosphate fertilizer treatment (HAP); (4) physical blending humic acid phosphate fertilizer treatment (HA+P); (5) market humic acid phosphate fertilizer treatment (SHAP, Sinochem Fertilizer Co. Ltd., Beijing, China).

Tomato seeds (Jingfan 308F₁) were sterilized with 10% H_2O_2 for 30 min and incubated in warm broth in a water bath at 35 °C for 2 h, followed by dark incubation in a light incubator until the seeds showed white. The seeds were incubated at 27 °C and 60% humidity. After germination, seedlings were sown in the substrate for seedling development. The soil was dried, ground, and sieved. Urea and potassium sulfate ($\text{N}:0.2 \text{ g}\cdot\text{kg}^{-1}$,

K₂O:0.15 g·kg⁻¹ soil) were mixed into the soil at the same time, and phosphorus fertilizer for the test was placed in a dialysis bag according to the principle of equal phosphorus amount (P₂O₅:0.15 g·kg⁻¹ soil) and buried in the soil. The tomato seedlings were transplanted after 10 days of growth. Normal water management was carried out daily, and plants were harvested after 40 days of growth.

2.2.2. Sampling and Test Methods

The residual materials in the HA+P- and HAP-treated dialysis bags were collected and characterized. Rhizosphere soil samples from the 5th, 12th, 22nd, and 40th days of tomato culture were dried, ground, and screened. The content of available phosphorus in soil was determined via 0.5 mol·L⁻¹ NaHCO₃ extraction and the molybdenum–antimony resistance colorimetric method. Fresh soil samples collected on the 5th and 40th days of HAP and HA+P treatments were stored at −20 °C for DNA extraction, and high-throughput sequencing, and bioinformatic analysis of microbial community. Rhizosphere soil samples collected by HA+P and HAP on the 5th day were denoted as HA+P5 and HAP5, respectively, and rhizosphere soil samples which were collected on the 40th day were denoted as HA+P40 and HAP40, respectively.

The above-ground part of tomato plant samples was separated from the underground part. After washing and drying, the biomass indexes such as seedling height, stem diameter and dry weight were measured. The dried samples were boiled with H₂SO₄-H₂O₂, and the total nitrogen content of plants was determined by Kjeldahl method. The content of total phosphorus was determined by molybdenum-antimony resistance colorimetry. The content of total potassium in plants was determined by flame spectrophotometry.

2.3. Characterization Methods

Scanning electron microscopy-Energy dispersive spectrometer. The surface morphologies of HA+P and HAP residues were scanned using a scanning electron microscope (Hitachi S-4800), and the self-contained energy spectrometer analyzed HA+P and HAP residues to determine elemental composition.

Fourier-transform infrared spectroscopy. The functional group structure of the test phosphate fertilizer was analyzed using an infrared spectrometer (Bruker VERTEX 70). Test conditions: approximately 2 mg of sample and 200 mg of potassium bromide were mixed and pressed, and the infrared spectral characteristics of the sample in the wave number range 4000–400 cm⁻¹ were recorded using an FT-IR spectrometer. Baseline correction of the spectra and data smoothing correction were performed using OMINC 8.2 software. Plotting was performed using Origin 2018 software.

X-ray photoelectron spectroscopy. XPS (Thermo Scientific K-Alpha, the United States of America) was used to characterize the composition of HA+P and HAP residue materials as well as the chemical state of each component and to quantitatively analyze the content of each component.

Solid-state ¹³C-nuclear magnetic resonance spectroscopy. The detailed distribution of HA+P and HAP residues' carbon functional groups was elucidated via NMR technique (Bruker 400 M). The carbon types were divided into alkyl carbons (C_{Alk}, 0–65 ppm), O-alkyl carbons (C_{Alk-O}, 65–100 ppm), aromatic carbon (C_{Ar-H,R}, 100–140 ppm), O-aromatic carbon (C_{Ar-O}, 140–156 ppm), carboxyl carbon (C_{COO-H,R}, 156–190 ppm), and carbonyl carbon (C_{C=O}, 190–250 ppm) [29,30].

2.4. High-Throughput Sequencing and Bioinformatic Analysis of Microbial Community

The detection of soil microbial community was performed according to previous study [31]. Soil total DNA was extracted from 0.5 g of fresh soil using a FastDNA Spin Kit for Soil (MP Biomedicals, Santa Ana, CA, USA). Primer sets 799F/1193R and ITS1f/ITS2 were used for PCR amplification of the V5-V7 region of bacterial 16S rRNA gene and the ITS (internal transcribed spacer) of fungal rRNA genes, respectively. The 25-μL PCR system contained 12.5 μL PCR premix (ExTaqTM; Takara, Shiga, Japan), 0.5 μL (10 μm)

of the forward and reverse primers, 0.5 μL DNA template (20 ng/ μL), and 11 μL sterile double-distilled water. PCR was performed with the thermocycle of initial denaturation at 94 $^{\circ}\text{C}$ for 10 min, 30 cycles of denaturation at 94 $^{\circ}\text{C}$ for 30 s, annealing at 55 $^{\circ}\text{C}$ /56 $^{\circ}\text{C}$ (16S rRNA/ITS) for 45 s, extension at 72 $^{\circ}\text{C}$ for 1 min, and a final extension at 72 $^{\circ}\text{C}$ for 10 min. High-throughput sequencing of the PCR products was performed using the Illumina HiSeq2000 platform (Illumina, San Diego, CA, USA).

Bioinformatic analysis was performed using the VSEARCH package (version 2.21.1) as described in previous studies [32,33]. Briefly, the paired-end reads were merged, and low-quality sequences (errors per base greater than 0.001 or length < 150 bp) were filtered. Next, chimeric reads were detected and removed using the UCHIME algorithm (uchime3_denovo). Then the high-quality reads were denoised using the UNOISE algorithm (version 3), and ZOTUs (zero-radius operational taxonomic units) were generated. Taxonomic assignment of the ZOTUs was performed using a Sintax algorithm [34] based on the reference of the SILVA rRNA database (version 138) and the UNITE database (version 8.3). After removing the ZOTUs that could not be assigned as bacteria or fungi, bacterial and fungal OTU tables were rarefied to 130,000 and 85,000 reads per sample, respectively, for downstream analysis.

PICTUS_{t2} [35] (phylogenetic investigation of communities through reconstruction of unobserved states) was used to predict the functional profiles of the bacterial community. The genes involved in P transformation were selected to detect bacterial phosphorus transformation functional potential [36].

2.5. Calculation and Statistical Analysis

The characterization results were analyzed using corresponding software. Data statistical analysis was performed using the R package (version 4.2.2) as described in previous studies [37,38]. One-way ANOVA was used to detect the significance of differences between treatments. Principal coordinate analysis (PCoA) based on Bray–Curtis distance was performed using a “vegan” library to show the difference between microbial communities under different P treatments. α diversity of microbial communities was determined using a “vegan” library. IBM Statistics SPSS 22.0 software (Duncan) was used, and all data were the means of three observations. Origin 2022 was used for illustration.

3. Results and Discussion

3.1. Structural Characterization of Synthetic Fertilizers

Figure 1 shows the surface morphology of HA+P and HAP. Under different magnification electron microscopy scans, HA+P and HAP showed some differences, with a smoother surface compared to HAP, and both exhibited loose and rich pore structures which were similar to the structure of humic acid previously reported in the literature [39,40]. Comparing HA+P and HAP by magnifying the image 20,000 times, HAP has more mesh structure on its surface and more mineral particles attached. Many depressed pores were formed on its surface under the effect of high-temperature reaction. The results showed that the chemical binding process of HA+P with phosphate fertilizer increased the surface area of HAP and revealed more binding sites, while its amorphous structure was well preserved.

In addition, we also characterized synthetic materials using infrared spectroscopy. Figure 2 shows the FT-IR spectra of P, HA+P, and HAP fertilizers. The FT-IR spectra of all three fertilizers are similar. The peaks at 3415 cm^{-1} are caused by the stretching of the -OH in alcohol and phenols. The peaks at 2489 cm^{-1} are skewed because of the stretching of PO-H, and the peak at 1631 cm^{-1} is shifted to 1654 cm^{-1} due to the vibration stretching of the -COOH. Moreover, HAP produced a new vibrational peak at 1101 cm^{-1} compared to P and HA+P, indicating the formation of a new chemical bond, -O-. The vibrational intensity of the peak of HAP at 980–500 cm^{-1} was lower than those of the other two materials, indicating the reduction of ash content in HAP. These FT-IR spectroscopy results show that the main functional groups of humic acid were not changed during the high-temperature

preparation of HAP, and new chemical bonds -O- were generated through bond cleavage and generation, which combined with phosphorus molecules to form phospholipid bonds.

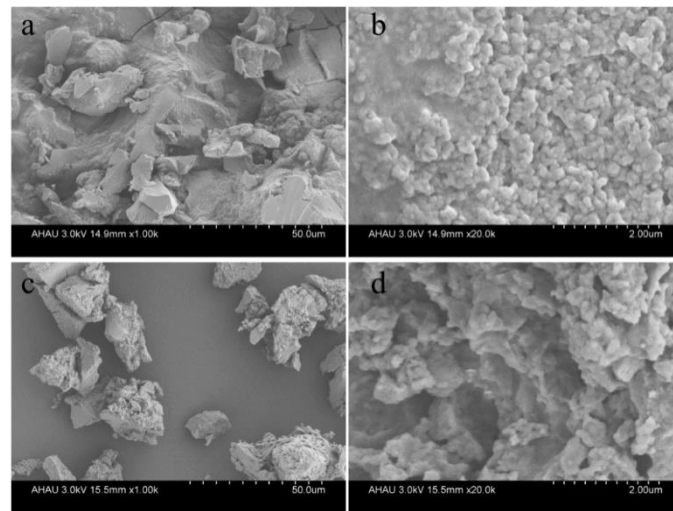


Figure 1. SEM images of HA+P and HAP. (a,b) HA+P magnified 1000 and 20,000 times, respectively; (c,d) HAP magnified 1000 and 20,000 times, respectively.

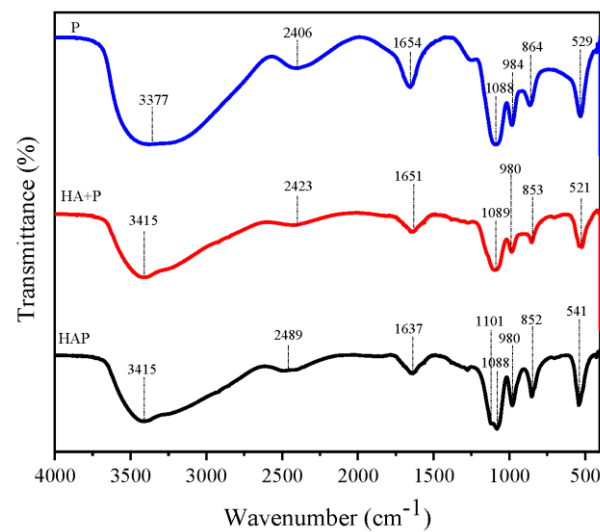


Figure 2. Fourier-transform infrared (FT-IR) spectra of P, HA+P, and HAP.

3.2. Mechanism of Chemical Synergistic Effect of Humic acid Phosphate Fertilizer on Phosphorus Availability

It can be observed from Figure 3 that the addition of humic acid had a greater effect on the available phosphorus content of the soil, showing a trend of first increasing and then decreasing, which is consistent with the nutrient release law of phosphorus in the soil. It was significantly increased compared to the application of common phosphorus fertilizer alone, which is because humic acid contains a variety of functional groups with strong ion exchange and adsorption ability, which can activate insoluble phosphorus in soil and increase the effectiveness of phosphorus [41]. The HAP treatment reached significant levels at different sampling periods, increasing by 13.8%, 21.2%, 47.7%, and 28.7% compared to the HA+P treatment. Among them, the soil fast-acting phosphorus content reached a maximum in all treatments at day 12. The combination of humic acid with phosphorus fertilizer had a high EC value within the phosphorus fertilizer microdomain, which alleviated the direct decomposition of humic acid by microorganisms and also

affected the phosphorus effectiveness and the phosphorus uptake by plants [42]. The results showed that the application of humic acid phosphate fertilizer prepared with humic acid had an increased effect on phosphorus effectiveness in the soil.

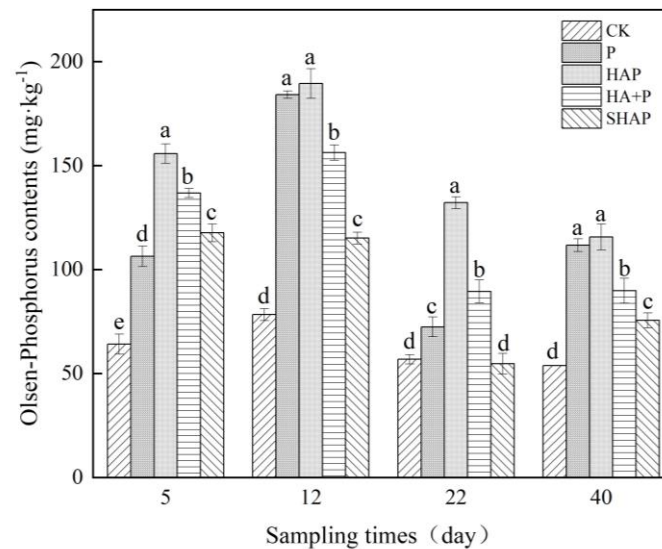


Figure 3. Changes of soil Olsen-P content under different treatments. Notes: Different lowercase letters indicate significant differences between treatments ($P < 0.05$).

Figure 4 shows the SEM-EDS diagram of the residue of the dialysis bag after pot culture of HA+P and HAP. Some humic acid pieces and particles can be seen from it. Both materials have rough surfaces, and HAP surface particles are small in size. The surface of HAP (Figure 4b) shows an aggregation state, which is caused by the reaction of functional groups on the HAP surface with mineral ions to form some complexes, resulting in the loading of more materials onto the HAP surface.

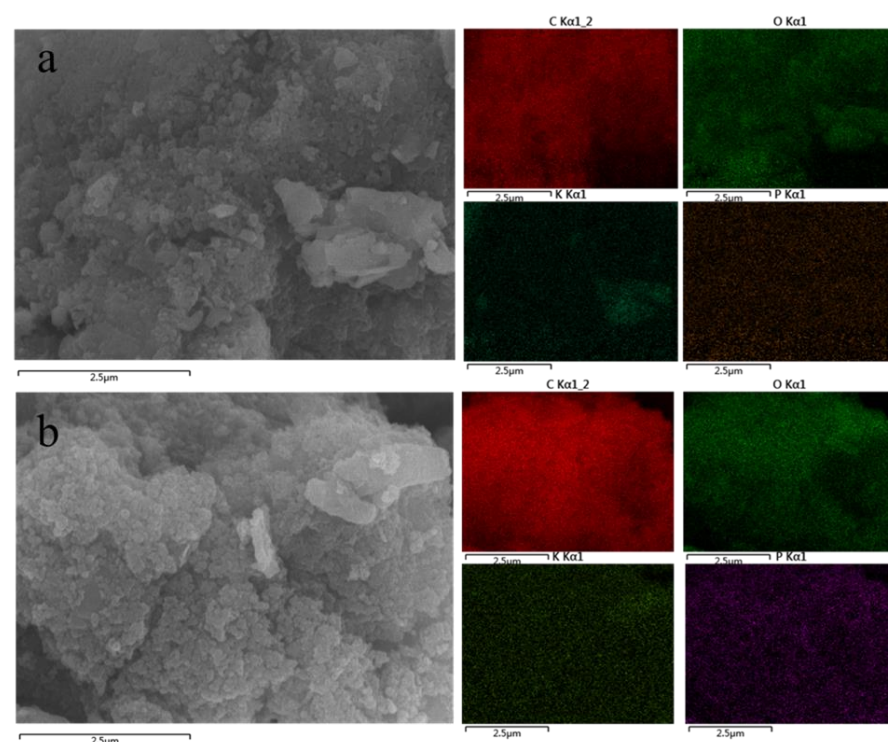


Figure 4. SEM and EDS images of HA+P (a) and HAP (b) residues of the dialysis bag after pot culture.

As can be seen from the EDS analysis diagram, the EDS microregion element analysis of the convex and concave points of the two materials contains C, O, K, and P, indicating that they are the composite parts of HA and potassium phosphate. The weight ratios of K and P in HAP are 2.9% and 0.3%, respectively, which are lower than that of HA+P (Table 1). After the application of chemical synthetic humic acid phosphate fertilizer in soil, a variety of physicochemical reactions caused the phosphate ester bond to break, release phosphorus, and increase the content of soil available phosphorus.

Table 1. Mass fraction of HA+P and HAP residue elements as percentages.

Treatments	Mass Fraction of HA+P and HAP Residue Elements (%)			
	C	O	K	P
HA+P	69.8	25.6	3.8	0.8
HAP	78.0	18.7	2.9	0.3

The FT-IR spectra of HA+P and HAP after soil incubation are shown in Figure 5. The strong and broad absorption peak at 3439 cm^{-1} is a hydroxyl group bonding stretching vibration. The bimodal peak near 2925 cm^{-1} represents the -CH stretching vibration of -CH₂ and -CH₃ in the aliphatic alkane structure [43], for which the intensity of the bimodal peak of HAP is significantly higher than that of HA+P, indicating that HAP has more aliphatic chains. The absorption peaks of the stretching vibration of C=O in the carboxyl and carbonyl groups are at 1617 cm^{-1} . The vibrational absorption peak of the phospholipid bond is around 1110 cm^{-1} . Presumably, the breakage of the phospholipid bond causes the disappearance of the absorption peak of HAP at 1114 cm^{-1} . The stretching vibration peak of (Si) O-H or (Ca, Mg, Fe, Al) with an -OH stretching vibration peak is 540 cm^{-1} [44].

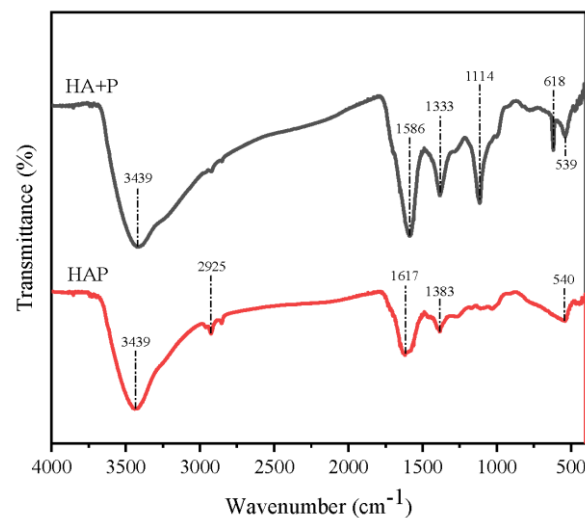


Figure 5. FT-IR spectra of HA+P and HAP treatment residues.

Figure 6 shows the solid-state ¹³C-NMR spectra of HA+P- and HAP-treated residues, and the carbon types of the two materials are analyzed. The spectral displacement peaks of HA+P and HAP are roughly the same, and the highest peaks occur at 100–140 ppm, indicating that the carbon types of the two materials mainly exist in the form of aromatic compounds. By integrating the peak areas of ¹³C-NMR spectra (Table 2), the alkyl carbon contents of HA+P and HAP are 8.04% and 7.51%, respectively; those of oxygen alkyl carbon are 1.64% and 1.44%, respectively; those of aromatic carbon are 63.86% and 63.22%, respectively; and those of aromatic C-O are 6.99% and 7.49%, respectively. Those of carboxyl/amide carbon are 12.87% and 13.66%, respectively, and those of carbonyl carbon were 6.60% and 6.68%, respectively. Compared to HA+P, the contents of alkyl carbon,

oxyalkyl carbon, and aromatic carbon in HAP treatment decreased by 0.53, 0.20, and 0.64 percentage points, respectively. The contents of aromatic C-O, carboxyl/amide carbon, and carbonyl carbon in HAP were higher than those in the HA+P treatment, and the content of carboxyl/amide carbon increased the most—by 0.79 percentage points. This indicates that more active functional groups are involved in the interaction with the phosphate ester, thus effectively preventing the fixation of phosphorus.

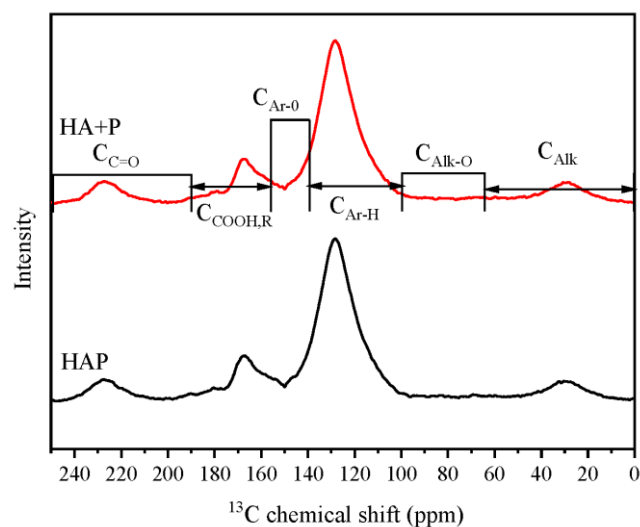


Figure 6. ^{13}C -NMR spectra of HA+P and HAP treatment residues.

Table 2. Relative contents of functional groups containing carbon in different displacement regions of HA+P and HAP.

Treatments	Relative Content of Functional Groups Containing Carbon (%)					
	C_{Alk} 0–65 ppm	$\text{C}_{\text{Alk-O}}$ 65–90 ppm	$\text{C}_{\text{Ar-H,R}}$ 90–140 ppm	$\text{C}_{\text{Ar-O}}$ 140–156 ppm	$\text{C}_{\text{COO-H,R}}$ 156–190 ppm	$\text{C}_{\text{C=O}}$ 190–250 ppm
HA+P	8.04	1.64	63.86	6.99	12.87	6.60
HAP	7.51	1.44	63.22	7.49	13.66	6.68

Four elements—C, O, K, and P—were detected in the XPS spectra of both HA+P and HAP (Figure 7a), which confirmed the presence of P and K in the reacted humic acid material. The XPS spectra were fitted to C1s, N1s, O1s, and P2p according to the literature as well as the humic acid characteristics [45].

Combined with the analysis of Figure 7b and Table 3, the P2p spectra of XPS all show three sub-peaks: 132.18 eV, 132.82 eV, and 133.66 eV in HA+P treatment and 132.26 eV, 133.10 eV, and 133.78 eV in HAP treatment. They are PO_4^{3-} , HPO_4^{2-} , and H_2PO_4^- , respectively [46,47]. The relative content of H_2PO_4^- in HAP treatment residues is 31.83%, which is 1.71% more than that in HA+P treatment residues, and the relative content of phosphate in HPO_4^{2-} is 38.95%, which is 6.99% less than that in HA+P treatment residues. The figure shows the C1s spectra of HA+P and HAP with binding energy peaks concentrated at 284.38, 284.78, 286.38, and 288.18 eV for HA+P and 284.48, 284.88, 286.38, and 287.88 eV for HAP, which can be assigned to C-C, C-H, C-O, and C=O, respectively. The fitted N1s peaks for HA+P and HAP appear in pyrrole N-5 and pyridine N-6, with binding energies of 400.28 and 400.18 eV, respectively, for pyrrole N-5 and of 399.18 eV for both for pyridine N-6. The O1s spectrum of XPS confirmed that HAP has more C=O as carboxyl groups, while no hydroxyl groups were detected in HAP—probably due to the high-temperature reaction producing bond breakage and generating new bonds, which is consistent with the FT-IR results—while the carboxyl group in humic acid may complex with metal ions and phosphate ions to form HA-M-P complexes. The results

showed that different binding processes of humic acid phosphate fertilizer could effectively activate insoluble phosphate in soil and that the availability of soil phosphorus could be changed through morphological transformation [48]. Soluble phosphate ($H_2PO_4^-$) content in HAP treatment was higher, and the promotion effect of HAP treatment on phosphorus availability was more significant than that of HA+P.

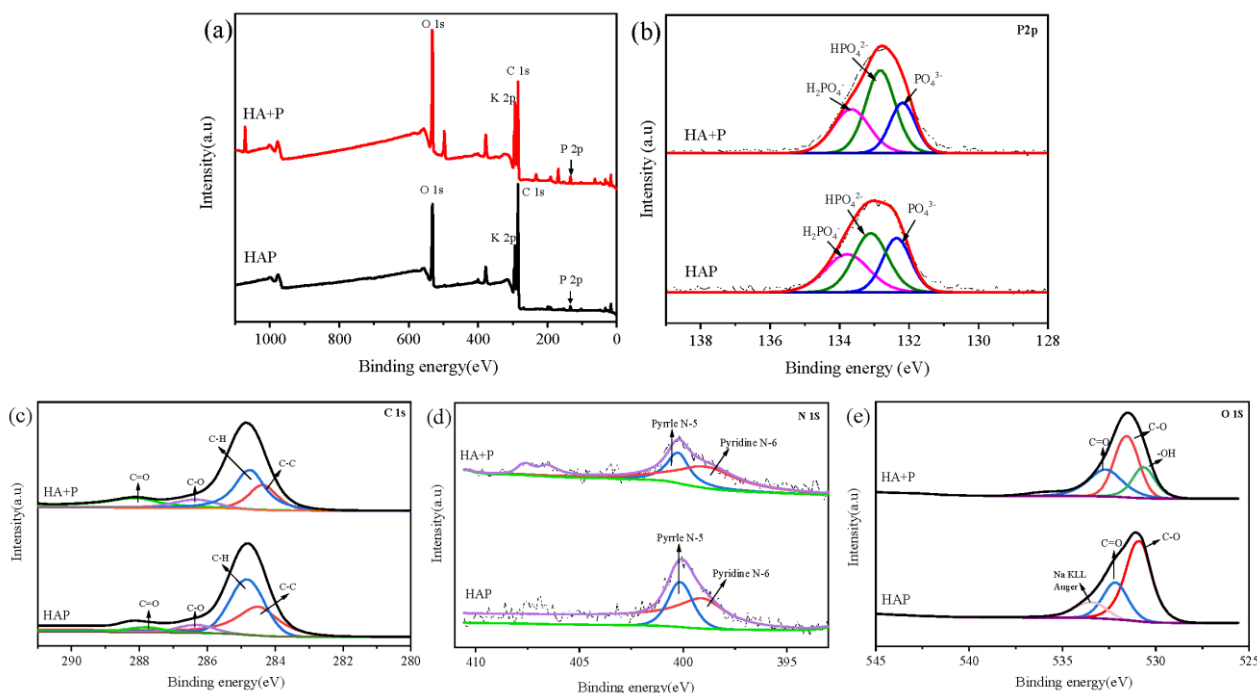


Figure 7. XPS spectra (a); P 2p (b), C1s (c), N1s (d), and O1s (e) spectra of HA+P and HAP residues.

Table 3. Relative contents of different phosphorus forms in P 2p spectra as percentages.

P Type	HA+P		HAP	
	Binding Energy (eV)	Relative Content (%)	Binding Energy (eV)	Relative Content (%)
$H_2PO_4^-$	133.66	30.12	133.78	31.83
HPO_4^{2-}	132.82	45.94	133.10	38.95
PO_4^{3-}	132.18	23.94	132.26	29.22

3.3. Biological Enhancement Mechanism of Phosphorus Effectiveness by Humic Acid Phosphate Fertilizer

Bacterial communities in the study’s soil were primarily constituted by *Myxococcota*, *Planctomycetota*, *Verrucomicrobiota*, *Firmicutes*, *Gemmatimonadota*, *Chloroflexi*, *Actinobacteriota*, *Acidobacteriota*, *Bacteroidota*, and *Proteobacteria*, which accounted for 97.02% (HA+P5), 96.75% (HAP5), 95.30% (HA+P40), and 96.49% (HAP40) of the total community, respectively, in relative abundance from Figure 8. However, the relative abundance of these taxa varied between different treatments and incubation stages. The variation of microbial community between HA+P and HAP treatments is further depicted by the 2D plot of PCoA. At the early incubation stage, soil bacterial communities in HA+P and HAP were clustered together, showing the high similarity of bacterial communities in the two treatments. However, after 40 days of incubation, the two treatments were separated from each other clearly, indicating the great variation of the bacterial communities. These results showed that although bacterial taxonomic composition varied little under different treatments, bacterial community structures were distinctly impacted by different treatments.

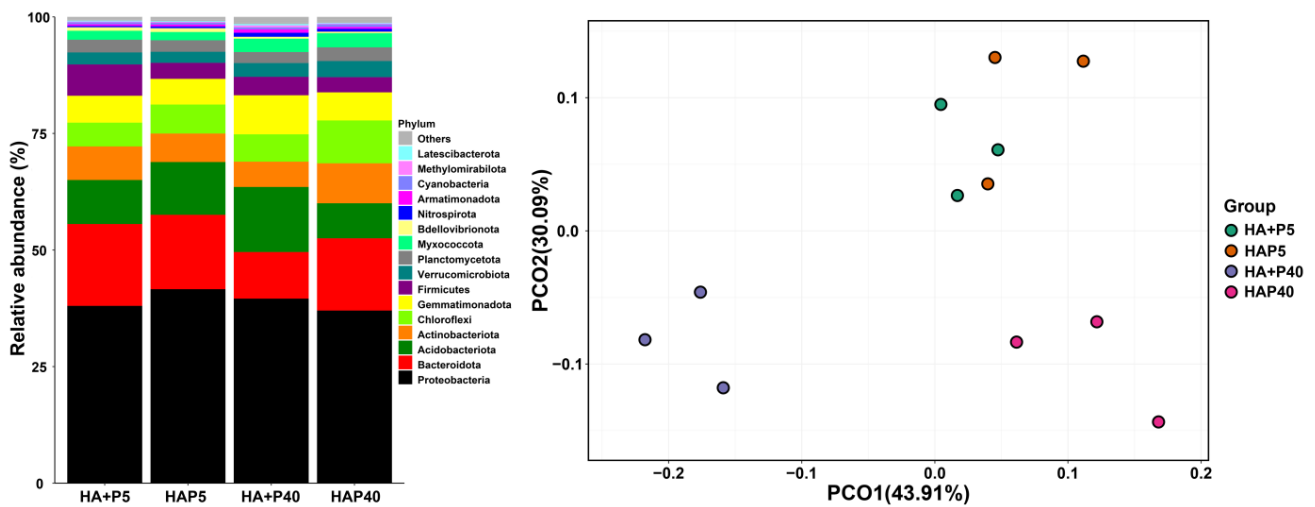


Figure 8. Soil microbial bacterial composition and PCoA plot showing the variation of community structure.

Microbes are the primary drivers for soil P transformation [49]. The results of functional prediction showed the different impacts of HA+P and HAP on bacterial functional profiles involved in P transformation (Figure 9). For single genes encoding organic phosphorus mineralization and inorganic phosphorus solubilization processes, the combination of humic acid and phosphate fertilizer chemistry in the soil increased the number of phytase and PQQGDH genes compared to the HA+P treatment ($P < 0.01$). The number of genes encoding alkaline phosphatase was increased by 3.23% (The HAP and HA+P treatments' numbers of genes were 60,327 and 58,439, respectively) compared to HA+P treatment. The results showed that the addition of HAP increased the number of microorganisms related to phosphorus transformation in the soil, which may be due to the fact that humic acid fertilizers promote the growth and development of crop roots, increase the number of crop roots and their exudates [50,51], and improve the soil microenvironment, thus increasing the number of microorganisms in the soil.

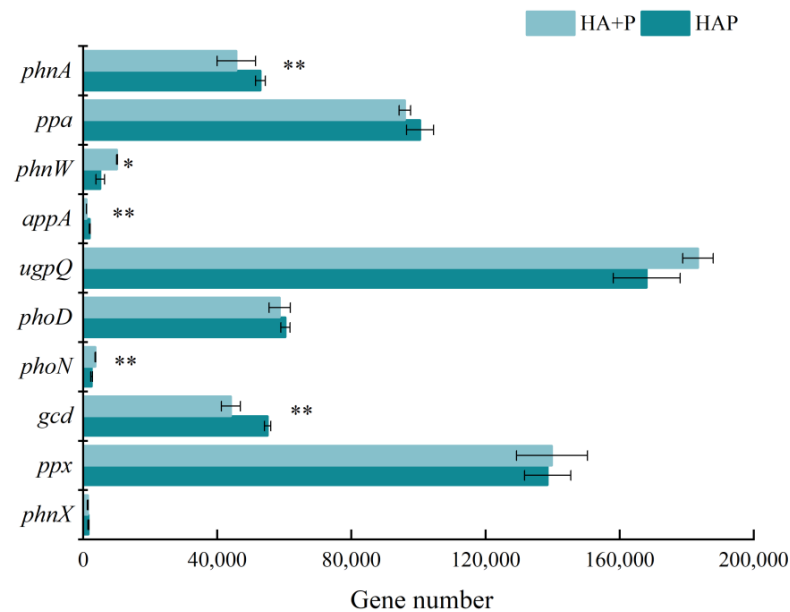


Figure 9. The abundance of genes involved in inorganic P solubilization and organic P mineralization in soil at 40 days after HA+P and HAP culture determined by PICRUST2. * and ** indicate significant differences between HA+P and HAP treatments (** $P < 0.01$, * $P < 0.05$).

3.4. Growth and Nutrient Absorption Analysis of Tomato Plants

Baghaie et al. [52] showed that the addition of humic acid could improve the nutritional quality and fruit yield of tomato plants but did not investigate whether structural changes in the combination of HAP could promote the growth of tomato seedlings. In this study, the application of phosphorus fertilizer could promote the growth of tomato seedlings and increase their plant height, stem diameter, and biomass (Table 4). Compared to CK, plant height after HA+P and HAP treatment increased by 10.3% and 21.3%, respectively, and HAP treatment showed a significant difference ($P < 0.05$). Stem diameter with HAP treatment was 15.31% higher than that of CK treatment, but the difference was not significant ($P > 0.05$). HAP dry weight increased by 61.02% and 177.18%, respectively, which were significantly higher than those of CK treatment ($P < 0.05$). Under the same humic acid addition concentration, HA+P and HAP treatments had similar stimulation effects on tomato plants, but there was no significant difference between them ($P > 0.05$). In addition, as can be seen from Figure 10, stem and leaf forks of tomatoes treated with HAP are more numerous, and their growth status is obviously better than that of other treatments.

Table 4. Effects of different treatments on plant height, stem diameter, and biomass of tomato plants.

Treatments	Plant Height (cm)	Stem Diameter (cm)	Biomass (g·Plant ⁻¹)	
			Shoot	Root
CK	36.95 ± 3.35 b	6.27 ± 0.70 a	3.31 ± 0.31 b	0.18 ± 0.05 b
P	41.10 ± 0.70 ab	7.33 ± 0.68 a	5.20 ± 0.69 a	0.44 ± 0.14 a
HAP	44.83 ± 1.46 a	7.23 ± 0.51 a	5.33 ± 1.33 a	0.50 ± 0.05 a
HA+P	40.77 ± 2.06 ab	6.37 ± 2.00 a	4.70 ± 0.31 ab	0.34 ± 0.10 ab
SHAP	42.10 ± 3.32 a	6.50 ± 0.53 a	4.87 ± 0.73 a	0.36 ± 0.12 ab

Notes: Different lowercase letters indicate significant differences between treatments ($P < 0.05$).



Figure 10. Growth of tomato plants under different treatments.

The application of P fertilizer was beneficial to the accumulation of plant nutrients, and the contents of P and K in the above-ground and underground parts of tomato plants were increased by each P application treatment, but there was no significant effect on the nitrogen content in each part of tomato plants ($P > 0.05$) (Table 5). Compared to other phosphorus application treatments, HAP promoted the absorption of P and K elements more significantly in tomatoes, and the accumulations of P and K elements in the shoot reached 1.49 g·plant⁻¹ and 16.05 g·plant⁻¹, respectively, which are consistent with the results of Jing et al. [27]. HAP treatment had the highest phosphorus accumulation in the ground. The phosphorus uptake of tomato under SHAP treatment was the highest (2.50 g·plant⁻¹), which was significantly increased by 38.89% compared to the CK treatment ($P < 0.05$), but there was no significant difference between other treatments and the CK treatment ($P > 0.05$). Humic acid can stimulate the root growth of crops, which is related to the auxin-like effect of humic acid, which promotes the absorption of nutrients by promoting root elongation [53]. However, the accumulation effect of phosphorus in the

underground part of tomato treated with SHAP is more significant, which may be because the synthesis technology of humic acid phosphate fertilizer on the market is more mature, and the trace elements in the synthesis process will also affect the root growth and nutrient absorption of plants [54].

Table 5. Accumulation of N, P, and K elements in tomato plants under different treatments.

Treatments	Plant Underground Part			Plant Above-Ground Part		
	N Accumulation (g·Plant ⁻¹)	P Accumulation (g·Plant ⁻¹)	K Accumulation (g·Plant ⁻¹)	N Accumulation (g·Plant ⁻¹)	P Accumulation (g·Plant ⁻¹)	K Accumulation (g·Plant ⁻¹)
CK	0.82 ± 0.10 ab	0.77 ± 0.23 c	5.53 ± 2.86 b	0.67 ± 0.21 a	1.80 ± 0.17 b	26.14 ± 1.20 a
P	0.82 ± 0.04 ab	1.22 ± 0.13 ab	15.12 ± 5.92 a	0.78 ± 0.02 a	1.85 ± 0.18 b	28.69 ± 2.06 a
HAP	0.82 ± 0.03 ab	1.49 ± 0.24 a	16.05 ± 1.44 a	0.77 ± 0.01 a	1.88 ± 0.21 b	28.73 ± 1.49 a
HA+P	0.90 ± 0.02 a	1.17 ± 0.17 abc	12.76 ± 2.89 ab	0.78 ± 0.01 a	1.92 ± 0.21 b	27.89 ± 2.01 a
SHAP	0.79 ± 0.03 b	0.93 ± 0.32 bc	12.59 ± 5.27 ab	0.70 ± 0.20 a	2.50 ± 0.35 a	29.9 ± 2.82 a

Notes: Different lowercase letters indicate significant differences between treatments ($P < 0.05$).

4. Discussion

The form of phosphorus in soil is closely related to its availability. The FT-IR spectra of chemically synthesized humic acid phosphate fertilizer (HAP) prepared in this study showed a new absorption peak at 1088 cm⁻¹, which was inferred to be the formation of -O-, which combined with phosphoric acid to form a phosphate ester (P-O-C) structure. It is believed that through physical or chemical interaction, humic acid and phosphorus fertilizer could form new phosphorus forms that could not be fixed easily, thus improving the availability of phosphorus. In this study, HAP treatment increased the soil available P content by 13.8–47.7% compared to HA+P treatment at different periods, indicating that chemical synthesis of humic acid phosphate fertilizer was more effective in improving the availability of soil phosphorus in the fertilizer sphere. This may be related to the double decomposition reaction between humic acid and phosphate, which was proven by the double decomposition reaction between humic acid and ammonium phosphate, which promoted the phosphoric acid in insoluble calcium phosphate and calcium dihydrogen phosphate to become water-soluble ammonium phosphate and phosphoric acid and improved the availability of phosphorus.

XPS analysis results of fertilizer residues showed that HAP treatment did not detect the presence of hydroxyl or that the content of hydroxyl was very low. ¹³C-NMR results showed that the contents of aromatic C-O, carboxyl/amide carbon, and carbonyl carbon with high activity oxygen functional groups increased significantly, while the content of alkyl carbon, oxyalkyl carbon, and aromatic carbon decreased. This may all be related to the process of the high-temperature preparation of phosphate fertilizer. The temperature rises abruptly due to acid–base neutralization, and the hydroxyl group in humic acid reacts with phosphoric acid [55]. In this study, O1s of X-ray photoelectron spectroscopy confirmed that HAP had more C=O, and precise analysis of phosphorus morphology of phosphate residues by XPS revealed that HAP treatment had 1.71% more H₂PO₄⁻ than HA+P treatment. All the above results indicate that the soluble phosphate content in HAP treatment residues was higher. The carboxyl group in humic acid may be complexed with calcium ions and phosphate ions to form a HA-M-P complex, which reduces the fixation of phosphorus by metal ions and increases the content of soluble phosphate, which is conducive to absorption by tomatoes. Gerke [56] and Erro et al. [57] found that humic acid can chelate iron, calcium, and other metal ions and form ternary complexes with phosphate to maintain high bioavailability and reduce the fixation of phosphorus. In short, increasing organophosphates can reduce the fixation of orthophosphate by metal ions, and the formation of HA-M-P complex by complexation is conducive to absorption and utilization by plants. These two methods can not only reduce the fixation of phosphorus but also be easily absorbed and utilized by plants.

Humic acid can significantly activate soil and improve the quantity and diversity of soil microorganisms. Soil microorganisms directly or indirectly participate in almost all biological and chemical reactions in soil, and their quantity, type, and related enzyme activities are directly related to soil quality [50]. It has been reported that the application of humic acid phosphate fertilizer can significantly affect the bacterial community's structure. The results of this study are consistent with those of previous studies. The application of humic acid phosphate fertilizer with different combination technologies can improve the species abundance and quantity of soil rhizosphere microorganisms and also change the bacterial microbial community's structure. The relative abundances of *Proteobacteria*, *Acidobacteriota*, *Gemmatimonadota*, and *Firmicutes* were changed. In this study, a large number of genes related to organic phosphate mineralization and inorganic phosphorus dissolution were expressed. Meanwhile, the metabolome analysis of soil microorganisms showed that the number of genes encoding phytase and alkaline phosphatase increased by 3.23% (number of ppa genes) and 2.90% (number of phoD genes) compared to HA+P treatment. The mineralization of organophosphorus is inseparable from microorganisms. The results of this study indicated that humic acid phosphate fertilizer mainly promoted the utilization of organophosphorus such as phosphate ester by soil microorganisms.

In this study, no matter how humic acid was combined with phosphorus fertilizer, it promoted the growth of tomato plants and increased plant height, stem diameter, and biomass. Compared to the control, plant height, stem diameter, and above-ground and underground biomass of HAP-treated tomato increased by 21.3%, 15.31%, 61.02%, and 177.18%, respectively. Izhar et al. [2] also came to the same conclusion when exploring the influence of humic acid on wheat growth. Humic acid can promote the growth of plants not only in the above-ground part of the plant but also in root growth and nutrient absorption. Humic acid phosphate fertilizer with different combination techniques could promote the accumulation of nutrient elements in tomatoes. The total accumulation of N, P, and K in HAP treatment was increased by 6.71%, 31.13%, and 41.40%, respectively, compared to the control treatment. In conclusion, the effects of chemically synthesized phosphorus humate (HAP) fertilizer on tomato growth and nutrient absorption can be attributed to the following reasons: by changing the chemical structure of phosphorus fertilizer, the transformation of phosphorus form in soil was promoted, the content of H_2PO_4^- phosphorus was increased, and the soil's nutrient status was improved. HAP changes the rhizosphere soil microbial community structure, promotes organic phosphate mineralization and then promotes tomato root growth and nutrient absorption.

5. Conclusions

The high temperature generated during the preparation of humic acid phosphate fertilizer (HAP) induces structural changes in humic acid, resulting in the formation of new chemical bonds (-O-) between humic acid and phosphate. This process leads to the formation of phosphate esters, an increased specific surface area of humic acid, and the exposure of additional binding sites. Consequently, the formation of HA-M-P complexes occurs, which slows down the release of phosphorus in the soil and reduces its fixation. These mechanisms contribute to the enhanced effectiveness of phosphorus. Furthermore, humic acid stimulates the growth and uptake of nitrogen (N), phosphorus (P), and potassium (K) by tomato seedlings. The combined use of HAP with phosphorus fertilizer yields the most significant results due to the formation of HA-M-P complexes, which further amplify phosphorus effectiveness. Additionally, humic acid enriches soil bacteria involved in phosphorus transformation, leading to increased soil phosphorus availability through enhanced phosphorus mineralization and solubilization. Future experiments will delve into the metabolic pathways through which microorganisms secrete relevant proteins to augment soil phosphorus effectiveness.

Author Contributions: Q.X. wrote the main paper; S.W. and Y.X. analyzed the samples; X.L. and L.Z. (Lei Zhang) collected the samples; Y.X. contributed to data interpretation; Q.X., X.C. and X.Y. designed the research; G.X., J.J., L.Z. (Ligan Zhang), D.T. and X.Y. polished the paper. All authors discussed the results and commented on the manuscript at all stages. All authors have read and agreed to the published version of the manuscript.

Funding: This work was financially supported by the National Key Technologies R&D Program of China during the 14th Five-Year Plan period (2023YFD1700205), The Science Foundation for Youth of Anhui Province (1908085QC139), Major Science and Technology in Anhui Province (202103a06020012), The Science Foundation for Distinguished Youth of Anhui Province (2008085J13), and the Key Project of the Educational Commission of Anhui Province of China (2022AH050886).

Data Availability Statement: Data are available upon request.

Conflicts of Interest: The authors declare no conflict of interest.

References

1. Kaya, C.; Şenbayram, M.; Akram, N.A.; Ashraf, M.; Alyemeni, M.N.; Ahmad, P. Sulfur-enriched leonardite and humic acid soil amendments enhance tolerance to drought and phosphorus deficiency stress in maize (*Zea mays* L.). *Sci. Rep.* **2020**, *10*, 6432. [[CrossRef](#)] [[PubMed](#)]
2. Izhar Shafi, M.; Adnan, M.; Fahad, S.; Wahid, F.; Khan, A.; Yue, Z.; Danish, S.; Zafar-ul-Hyu, M.; Brtnicky, M.; Datta, R. Application of Single Superphosphate with Humic Acid Improves the Growth, Yield and Phosphorus Uptake of Wheat (*Triticum aestivum* L.) in Calcareous Soil. *Agronomy* **2020**, *10*, 1224. [[CrossRef](#)]
3. Busato, J.G.; Ferrari, L.H.; Chagas Junior, A.F.; da Silva, D.B.; dos Santos Pereira, T.; de Paula A., M. Trichoderma strains accelerate maturation and increase available phosphorus during vermicomposting enriched with rock phosphate. *J. Appl. Microbiol.* **2021**, *130*, 1208–1216. [[CrossRef](#)]
4. Smith, W.F.; Mudge, R.S.; Rae, L.A.; Glassop, D. Phosphate transport in plants. *Plant and Soil* **2003**, *248*, 71–83. [[CrossRef](#)]
5. Cheng, L.Y.; Bucciarelli, B.; Shen, J.B.; Allan, D.; Vance, C.P. Update on whitelupin cluster root acclimation to phosphorus deficiency. *Plant Physiol.* **2011**, *156*, 1025–1032. [[CrossRef](#)]
6. Rashad, M.; Hafez, M.; Popov, A.I. Humic substances composition and properties as an environmentally sustainable system: A review and way forward to soil conservation. *J. Plant Nutr.* **2022**, *45*, 1072–1122. [[CrossRef](#)]
7. Ji, Q.-K.; Wang, D.; Yang, W.-B.; Han, Y.-R.; Ma, W.-Q.; Wei, J. Effects of long-term phosphorus application on crop yield, phosphorus absorption, and soil phosphorus accumulation in maize-wheat rotation system. *J. Appl. Ecol.* **2021**, *32*, 2469.
8. Hafez, M.; Popov, A.I.; Rashad, M. Evaluation of the effects of new environmental additives compared to mineral fertilizers on the leaching characteristics of some anions and cations under greenhouse plant growth of saline-sodic soils. *Open Agric. J.* **2020**, *14*, 246–256. [[CrossRef](#)]
9. Li, B.Y.; Zhou, D.M.; Cang, L.; Zhang, H.L.; Fan, X.H.; Qin, S.W. Soil micronutrient availability to crops as affected by long-term inorganic and organic fertilizer applications. *Soil Tillage Res.* **2007**, *96*, 166–173. [[CrossRef](#)]
10. Barrow, N.J. Soil phosphate chemistry and the P-sparing effect of previous phosphate applications. *Plant Soil* **2015**, *397*, 401–409. [[CrossRef](#)]
11. Balemi, T.; Negisho, K. Management of soil phosphorus and plant adaptation mechanisms to phosphorus stress for sustainable crop production: A review. *J. Soil Sci. Plant Nutr.* **2012**, *12*, 547–561. [[CrossRef](#)]
12. Mpanga, I.K.; Ludewig, U.; Dapaah, H.K.; Neumann, G. Acquisition of rock phosphate by combined application of ammonium fertilizers and *Bacillus amyloliquefaciens* FZB42 in maize as affected by soil pH. *J. Appl. Microbiol.* **2020**, *129*, 947–957. [[CrossRef](#)]
13. Tian, D.; Li, Z.; O'Connor, D.; Shen, Z.; Hou, D. The need to prioritize sustainable phosphate-based fertilizers. *Soil Use Manag.* **2020**, *36*, 351. [[CrossRef](#)]
14. Heuer, S.; Gaxiola, R.; Schilling, R.; Herrera-Estrella, L.; López-Arredondo, D. Wissuwa, M.; Delhaize, E.; Rouached, H. Improving phosphorus use efficiency: A complex trait with emerging opportunities. *Plant J.* **2017**, *90*, 868–885. [[CrossRef](#)] [[PubMed](#)]
15. Zhu, J.; Li, M.; Whelan, M. Phosphorus activators contribute to legacy phosphorus availability in agricultural soils: A review. *Sci. Total Environ.* **2017**, *612*, 522–537. [[CrossRef](#)]
16. Zhang, S.; Yuan, L.; Li, Y.; Zhao, B. Characterization of ultrafiltration-fractionated humic acid derived from chinese weathered coal by spectroscopic techniques. *Agronomy* **2021**, *11*, 2030. [[CrossRef](#)]
17. Guo, X.X.; Liu, H.T.; Wu, S.B. Humic substances developed during organic waste composting: Formation mechanisms, structural properties, and agronomic functions. *Sci. Total Environ.* **2019**, *662*, 501–510. [[CrossRef](#)]
18. Ghaderimokri, L.; Rezaei-Chiyaneh, E.; Ghiyasi, M.; Gheshlaghi, M.; Battaglia, M.L.; Siddique, K.H.M. Application of humic acid and biofertilizers changes oil and phenolic compounds of fennel and fenugreek in intercropping systems. *Sci. Rep.* **2022**, *12*, 5946. [[CrossRef](#)]
19. Zanin, L.; Tomasi, N.; Cesco, S.; Varanini, Z.; Pinton, R. Humic Substances Contribute to Plant Iron Nutrition Acting as Chelators and Biostimulants. *Front. Plant Sci.* **2019**, *10*, 675. [[CrossRef](#)]

20. Yang, F.; Zhang, S.; Song, J.; Du, Q.; Li, G.; Tarakina, N.V.; Antonietti, M. Synthetic humic acids solubilize otherwise insoluble phosphates to improve soil fertility. *Angew. Chem. Int. Ed.* **2019**, *58*, 18813–18816. [[CrossRef](#)]
21. Tang, W.W.; Zeng, G.M.; Gong, J.L.; Liang, J.; Xu, P.; Zhang, C.; Huang, B.B. Impact of humic/fulvic acid on the removal of heavy metals from aqueous solutions using nanomaterials: A review. *Sci. Total Environ.* **2014**, *468–469*, 1014–1027. [[CrossRef](#)]
22. Olk, D.C.; Bloom, P.R.; Perdue, E.M.; McKnight, D.M.; Chen, Y.; Fahrenhorst, A.; Senesi, N.; Chin, Y.-P.; Schmitt-Kopplin, P.; Hertkorn, N.; et al. Environmental and agricultural relevance of humic fractions extracted by alkali from soils and natural waters. *J. Environ. Qual.* **2019**, *48*, 217–232. [[CrossRef](#)] [[PubMed](#)]
23. Sun, Q.; Liu, J.; Huo, L.; Li, Y.; Xia, L.; Zhou, Z.; Zhang, M.; Li, B. Humic acids derived from Leonardite to improve enzymatic activities and bioavailability of nutrients in a calcareous soil. *Int. J. Agric. Biol. Eng.* **2020**, *13*, 200–205. [[CrossRef](#)]
24. Calvo, P.; Nelson, L.; Klopper, J.W. Agricultural uses of plant biostimulants. *Plant Soil* **2014**, *383*, 3–41. [[CrossRef](#)]
25. Canellas, L.P.; Olivares, F.L.; Aguiar, N.O.; Jones, D.L.; Nebbioso, A.; Mazzei, P.; Piccolo, A. Humic and fulvic acids as biostimulants in horticulture. *Sci. Hortic.* **2015**, *196*, 15–27. [[CrossRef](#)]
26. Yang, X.; Chen, X.; Yang, X. Effect of organic matter on phosphorus adsorption and desorption in a black soil from Northeast China. *Soil Tillage Res.* **2019**, *187*, 85–91. [[CrossRef](#)]
27. Jing, J.; Zhang, S.; Yuan, L.; Li, Y.; Lin, Z.; Xiong, Q.; Zhao, B. Combining humic acid with phosphate fertilizer affects humic acid structure and its stimulating efficacy on the growth and nutrient uptake of maize seedlings. *Sci. Rep.* **2020**, *10*, 17502. [[CrossRef](#)] [[PubMed](#)]
28. Wu, Y.; Li, S.; Chen, G. Impact of humic acids on phosphorus retention and transport. *J. Soil Sci. Plant Nutr.* **2020**, *20*, 2431–2439. [[CrossRef](#)]
29. Lin, Y.; Muoroe, P.; Joseph, S.; Henderson, R.; Ziolkowski, A. Water extractable organic carbon in untreated and chemical treated biochars. *Chemosphere* **2012**, *87*, 151–157. [[CrossRef](#)]
30. Yan, L.J.; Bai, Y.H.; Zhao, R.F.; Li, F.; Xie, K. Correlation between coal structure and release of the two organic compounds during pyrolysis. *Fuel* **2015**, *145*, 12–17. [[CrossRef](#)]
31. Sun, R.; Niu, J.; Luo, B.; Wang, X.; Li, W.; Zhang, W.; Wang, F.; Zhang, C.; Ye, X. Substitution of manure for mineral P fertilizers increases P availability by enhancing microbial potential for organic P mineralization in greenhouse soil. *Front. Bioeng. Biotechnol.* **2022**, *10*, 1078226. [[CrossRef](#)]
32. Sun, R.; Wang, X.; Tian, Y.; Guo, Y.; Feng, X.; Sun, H.; Liu, X.; Liu, B. Long-term amelioration practices reshape the soil microbiome in a coastal saline soil and alter the richness and vertical distribution differently among bacterial, archaeal, and fungal communities. *Front. Microbiol.* **2022**, *12*, 4143. [[CrossRef](#)] [[PubMed](#)]
33. Sun, R.; Ding, J.; Li, H.; Wang, X.; Li, W.; Li, K.; Ye, X.; Sun, S. Mitigating nitrate leaching in cropland by enhancing microbial nitrate transformation through the addition of liquid biogas slurry. *Agric. Ecosyst. Environ.* **2023**, *345*, 108324. [[CrossRef](#)]
34. Sintax, E.R.C. A simple non-bayesian taxonomy classifier for 16S and ITS sequences/RC edgar. *bioRxiv*, 2016; bioRxiv:074161.
35. Douglas, G.M.; Maffei, V.J.; Zaneveld, J.R.; Yurgel, S.N.; Brown, J.R.; Taylor, C.M.; Huttenhower, C.; Langille, M.G.I. PICRUSt2 for prediction of metagenome functions. *Nat. Biotechnol.* **2020**, *38*, 685–688. [[CrossRef](#)]
36. Sun, R.; Zhang, W.; Liu, Y.; Yun, W.; Luo, B.; Chai, R.; Zhang, C.; Xiang, X.; Su, X. Changes in phosphorus mobilization and community assembly of bacterial and fungal communities in rice rhizosphere under phosphate deficiency. *Front. Microbiol.* **2022**, *13*, 953340. [[CrossRef](#)]
37. Sun, R.; Wang, F.; Hu, C.; Liu, B. Metagenomics reveals taxon-specific responses of the nitrogen-cycling microbial community to long-term nitrogen fertilization. *Soil Biol. Biochem.* **2021**, *156*, 108214. [[CrossRef](#)]
38. Sun, R.; Chen, Y.; Han, W.; Dong, W.; Zhang, Y.; Hu, C.; Liu, B.; Wang, F. Different contribution of species sorting and exogenous species immigration from manure to soil fungal diversity and community assemblage under long-term fertilization. *Soil Biol. Biochem.* **2020**, *151*, 108049. [[CrossRef](#)]
39. Joo, J.C.; Shackelford, C.D.; Reardon, K.F. Association of humic acid with metal (hydr)oxide-coated sands at solid–water interfaces. *J. Colloid Interface Sci.* **2008**, *317*, 424–433. [[CrossRef](#)] [[PubMed](#)]
40. Negre, M.; Leone, P.; Trichet, J.; Défarge, C.; Boero, V.; Gennari, M. Characterization of model soil colloids by cryo-scanning electron microscopy. *Geoderma* **2004**, *121*, 1–16. [[CrossRef](#)]
41. Sun, G.F.; Jin, J.Y.; Shi, Y.L. Advances in the effect of humic acid and modified lignin on availability to crops. *Chin. J. Soil Sci.* **2011**, *42*, 1003–1009.
42. Wang, X.L.; Liang, C.H.; Ma, Z.H.; Han, Y. Effects of phosphate and zeolite on the transformation of Cd speciation in Soil. *Environ. Sci.* **2015**, *36*, 1437–1444.
43. Nasir, S.; Sarfaraz, T.B.; Verheyen, T.V.; Chaffee, A.L. Structural elucidation of humic acids extracted from Pakistani lignite using spectroscopic and thermal degradative techniques. *Fuel Process Technol.* **2011**, *92*, 983–991. [[CrossRef](#)]
44. Zhang, Z.Q.; Gao, Q.; Xie, Z.L.; Yang, J.; Liu, J. Adsorption of nitrification inhibitor nitrapyrin by humic acid and fulvic acid in black soil: characteristics and mechanism. *RSC Adv.* **2020**, *11*, 114–123. [[CrossRef](#)] [[PubMed](#)]
45. Schild, B.D.; Marquardt, C.M. Analysis of Th(IV)-humate by XPS. *Radiochim. Acta* **2000**, *88*, 587–591. [[CrossRef](#)]
46. Huang, R.X.; Tang, Y.Z. Speciation dynamics of phosphorus during (Hydro)thermal treatments of sewage sludge. *Environ. Sci. Technol.* **2015**, *49*, 14466–14474. [[CrossRef](#)]
47. Qian, T.T.; Yang, Q.; Chu, F.J.D.; Dong, F.; Zhou, Y. Transformation of phosphorus in sewage sludge biochar mediated by a phosphate-solubilizing microorganism. *Chem. Eng. J.* **2018**, *359*, 1573–1580. [[CrossRef](#)]

48. Cao, N.; Chen, X.P.; Cui, Z.L.; Zhang, F. Change in soil available phosphorus in relation to the phosphorus budget in China. *Nutr. Cycl. Agroecosystems* **2012**, *94*, 161–170. [[CrossRef](#)]
49. Rosling, A.; Midgley, M.G.; Cheeke, T.; Urbina, H.; Fransson, P.; Phillips, R.P. Phosphorus cycling in deciduous forest soil differs between stands dominated by ecto- and arbuscular mycorrhizal trees. *New Phytol.* **2016**, *209*, 1184–1195. [[CrossRef](#)] [[PubMed](#)]
50. Fierer, N. Embracing the unknown: Disentangling the complexities of the soil microbiome. *Nat. Rev. Microbiol.* **2017**, *15*, 579–590. [[CrossRef](#)]
51. Zhou, L.P.; Yuan, L.; Zhao, B.Q.; Li, Y.; Lin, Z. Advances in research on the mechanism of humic acid promoting root growth of crops. *Humic. Acid* **2019**, *23*, 13–18.
52. Baghaie, A.H.; Aghili, F. Contribution of *Piriformospora indica* on improving the nutritional quality of greenhouse tomato and its resistance against Cu toxicity after humic acid addition to soil. *Environ. Sci. Pollut. Res. Int.* **2021**, *28*, 64572–64585. [[CrossRef](#)] [[PubMed](#)]
53. Canellas, L.P.; Dobbss, L.B.; Oliveira, A.L.; Chagas, J.G.; AAguiar, N.O.; Rumjanek, V.M.; Novotny, E.H.; Olivares, F.L.; Spaccini, R. Piccolo, A. Chemical properties of humic matter as related to induction of plant lateral roots. *Eur. J. Soil Sci.* **2012**, *63*, 315–324. [[CrossRef](#)]
54. Wojciula, A.; Wiater, J. Trace Elements in Consumer Plants. *J. Ecol. Eng.* **2019**, *20*, 252–256. [[CrossRef](#)]
55. Zhang, Y.; Zhang, S.; Yuan, L.; Li, Y.; Lin, Z.; Wang, L.; Zhao, B. Structure analysis of citric acid modified phosphorus fertilizer and its effect on fixation rate of water-soluble phosphorus. *Plant Nutr. Fertil. Sci.* **2021**, *27*, 878–885.
56. Gerke, J. Review Article: The effect of humic substances on phosphate and iron acquisition by higher plants: Qualitative and quantitative aspects. *J. Plant Nutr. Soil Sci.* **2021**, *184*, 329–338. [[CrossRef](#)]
57. Erro, J.; Urrutia, O.; Baigorri, R.; Aparicio-Tejo, P.; Irigoyen, I.; Storino, F.; Mandado, M.; Yvin, J.C.; Garcia-Mina, J.M. Organic complexed superphosphates (CSP): Physicochemical characterization and agronomical properties. *J. Agric. Food Chem.* **2012**, *60*, 2008–2017. [[CrossRef](#)]

Disclaimer/Publisher's Note: The statements, opinions and data contained in all publications are solely those of the individual author(s) and contributor(s) and not of MDPI and/or the editor(s). MDPI and/or the editor(s) disclaim responsibility for any injury to people or property resulting from any ideas, methods, instructions or products referred to in the content.